# A Systematic Methodology for Optimal Design of Two-Phase Micro-Channel Heat Sinks

**Weilin Qu**
Graduate Research Assistant
Student Member ASME
e-mail: quw@purdue.edu

**Issam Mudawar**[1]
Professor and Director
Fellow ASME
e-mail: mudawar@ecn.purdue.edu

Purdue University International Electronic Cooling Alliance (PUIECA),
Boiling and Two-Phase Flow Laboratory,
School of Mechanical Engineering,
Purdue University,
West Lafayette, IN 47907

*This study provides a comprehensive methodology for optimizing the design of a two-phase micro-channel heat sink. The heat sink parameters are grouped into geometrical parameters, operating parameters, and thermal/fluid parameters. The objective of the proposed methodology is to optimize micro-channel dimensions in pursuit of acceptable values for the thermal/fluid parameters corresponding to a given heat flux, coolant, and overall dimensions of the heat generating device to which the heat sink is attached. The proposed optimization methodology yields an acceptable design region encompassing all possible micro-channel dimensions corresponding to a prescribed coolant flow rate or pressure drop. The designer is left with the decision to select optimum channel dimensions that yield acceptable values of important thermal/fluid parameters that are easily predicted by the optimization procedure.* [DOI: 10.1115/1.2056571]

## Introduction

Thermal engineers in the electronics industry are facing unprecedented challenges of removing enormous amounts of heat from devices and packages, which are brought about by aggressive circuit integration and miniaturization. In fact, breakthroughs in many high-performance electronic systems are becoming increasingly dependent upon the ability to safely dissipate the waste heat, as the reliability and life span of electronics are both strongly influenced by temperature. Among only a handful of available high-performance cooling techniques, micro-channel heat sinks have recently emerged as a highly effective thermal solution for next generation high-power-density electronics.

Micro-channel heat sinks utilize a series of small parallel channels as liquid flow passages and are especially suited for applications involving the dissipation of large amounts of heat from a small area. Key merits of these heat sinks are low thermal resistance, small coolant inventory, and small heat sink mass and volume. Depending on whether the liquid coolant maintains liquid state or undergoes flow boiling inside the micro-channels, heat sinks can be classified as either single phase or two phase. Compared to their single-phase counterparts, two-phase heat sinks produce much higher convective heat transfer coefficients, reduce coolant flow rate requirements, and provide greater streamwise temperature uniformity.

Effective design of any novel thermal/fluid system is often a two-step process with different objectives achieved in each step. In the first step, research efforts are concentrated on acquiring a fundamental understanding of the transport characteristics of the system. Where computational methods are in question, a thorough experimental study is often undertaken, and experimental data are combined with mechanistic models to refine existing models or develop new predictive tools for accurate description of the transport characteristics of the system. Once reliable predictive tools are established and verified, attention is shifted to optimal design of the system, which is the main objective of the second step of the design process. This step involves selecting a system geometry that yields optimum performance under prescribed input conditions.

Application of this two-step process is clearly evident in recent single-phase micro-channel heat sink development efforts. Early studies in this area were mostly focused on experimental investigation of pressure drop and heat transfer characteristics [1–7]. Heat sinks with different substrate materials and geometries were fabricated and tested with different liquid coolants. Experimental data were compared to predictions of models or correlations that were developed earlier for macro-channel flows. Most studies, especially the more recent ones, revealed macro-channel predictive tools are highly effective at predicting the pressure drop and heat transfer characteristics of single-phase micro-channel heat sinks [7]. Later, studies on optimal design of these heat sinks became more widely available [8–11]. Using macro-channel models, heat sink geometry was optimized by minimizing the overall thermal resistance of the heat sink.

Research on two-phase micro-channel heat sinks is fairly recent. Most published studies in this area concern the fundamental understanding of micro-channel flow boiling, including boiling incipience [12,13], dominant flow patterns [14–16], hydrodynamic instability [17–20], pressure drop [20–26], heat transfer [21,26–30], and critical heat flux (CHF) [31–33]. Experimental investigations were performed and experimental data compared to the predictions of macro-channels models or correlations. These studies revealed channel size has a significant influence on flow boiling in micro-channels and, unlike single-phase heat sinks, predictions of macro-channel models and correlations showed appreciable deviation from experimental data. Several new predictive tools specifically tailored to micro-channel flow boiling were proposed thereafter [20,29,30,33]. So far, no studies have been published on optimal design of a two-phase micro-channel heat sink.

The present study was motivated by the lack of a systematic methodology to guide two-phase micro-channel heat sink design. A new methodology is proposed wherein key heat sink parameters and the best available predictive tools are first identified. Different performance characteristics of the heat sink are then examined to optimize micro-channel dimensions in pursuit of acceptable values for the thermal/fluid parameters corresponding to a given heat flux, coolant, and overall dimensions of the heat generating device to which the heat sink is attached.

## System Parameters and Predictive Tools

Figure 1 illustrates the construction of a two-phase micro-channel heat sink. The heat sink is composed of a base substrate and a cover plate. The base substrate is usually made from silicon

[1]Author to whom correspondence should be addressed. Tel. (765) 494-5705; fax (765) 494-0539

Contributed by the Electronic and Photonic Packaging Division of ASME for publication in the JOURNAL OF ELECTRONIC PACKAGING. Manuscript received February 25, 2004; final manuscript received December 17, 2004. Review conducted by: Guo-Quan Lu.

  

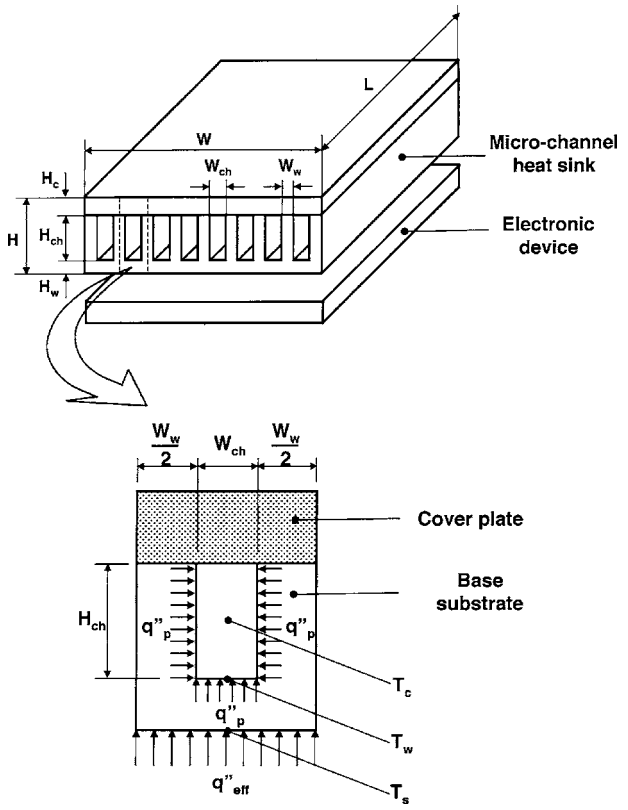


**Fig. 1 Construction of typical two-phase micro-channel heat sink**

or a high-thermal-conductivity metal such as copper or aluminum. A series of parallel micro-slots with characteristic dimensions ranging from 10 to 1000 $\mu$m are cut into the top surface of the base substrate. The cover plate is attached atop the base substrate to form rectangular micro-channels. While other channel geometries are possible, the rectangular geometry is often preferred for ease of fabrication. The cover plate is made from a low-thermal-conductivity material such as glass or high-temperature plastic to ensure that all the heat is removed by the coolant. The heat sink is attached to the top surface of a high-power-density electronic device as shown in Fig. 1. Heat generated by the device is conducted through the base substrate and removed by the coolant flowing through the micro-channels. Figure 1 shows a unit cell containing a single micro-channel and surrounding solid. Taking advantage of symmetry between micro-channels, the cooling performance of the heat sink can be derived from analysis of the unit cell alone.

A variety of system parameters must be examined when designing a two-phase micro-channel heat sink. As shown below, these parameters can be grouped into (1) geometrical parameters, (2) operating parameters, and (3) thermal/fluid parameters.

*Geometrical parameters* include heat sink and micro-channel dimensions and are illustrated in Fig. 1. The overall heat sink dimensions are length $L$, width $W$, and height $H$. When attaching a heat sink to an electronic device, the planform dimensions ($W \times L$) of the heat sink (excepting the inlet and outlet plenums) are often set equal to those of the device. Therefore, $L$ and $W$ are specified beforehand, and serve as input parameters for heat sink design. $H$ is the sum of cover plate thickness $H_c$, channel height $H_{ch}$, and distance between channel bottom wall and heat sink bottom wall $H_w$. Since the cover plate can be treated as thermally insulating, $H_c$ has no bearing on the overall heat sink performance. $H_w$, on the other hand, is proportional to the thermal conduction resistance between the electronic device and micro-channels and should be made as small as possible. In practice, there is always a practical minimum value for $H_w$ that is set by machining and/or structural limitations. Both $H_c$ and $H_w$ are excluded from present optimization methodology.

Aside from the planform dimensions ($W \times L$), the channel height $H_{ch}$, channel width $W_{ch}$, and wall thickness $W_w$ between neighboring channels constitute the primary geometrical parameters for heat sink design. The ultimate goal here is to select values for $H_{ch}$, $W_{ch}$, and $W_w$ that yield the most desirable heat sink performance. From Fig. 1, the number of channels in a heat sink can be evaluated from

$$N = \frac{W}{W_{ch} + W_w}. \tag{1}$$

*Operating parameters* represent conditions under which the heat sink is expected to operate. They include substrate material, type of coolant, inlet temperature $T_{in}$, outlet pressure $P_{out}$, total coolant volume flow rate $Q_t$, and heat flux $q''_{eff}$. $q''_{eff}$ represents the heat removal requirement of the heat sink and is based on the heat sink's planform area:

$$q''_{eff} = \frac{P_W}{WL}. \tag{2}$$

In heat sink design, another parameter $q''_p$ is often used to describe heat flux along the conducting walls of the micro-channels. Referring to Fig. 1, $q''_p$ can be related to $q''_{eff}$ by

$$q''_p = \frac{q''_{eff}(W_{ch} + W_W)}{W_{ch} + 2H_{ch}}. \tag{3}$$

Like heat sink overall dimensions, operating parameters also serve as input parameters in heat sink design, and their values are often specified beforehand.

*Thermal/fluid parameters* are dependent transport parameters that determine the performance of a heat sink under given geometrical and operating parameters. Key thermal/fluid parameters include pressure drop $\Delta P$, highest heat sink temperature $T_{max}$, minimum heat flux $q''_{min}$, and maximum heat flux $q''_{max}$. Given below is a discussion on how to evaluate each of these thermal/fluid parameters using the best available predictive tools.

**Pressure Drop $\Delta P$.** Pressure drop $\Delta P$ indicates the total pressure drop across a two-phase micro-channel heat sink. The magnitude of this parameter dictates the pumping power required to operate the heat sink and, in many cases, pump size and type.

For most two-phase micro-channel heat sink applications, liquid coolant is supplied into the heat sink in subcooled state ($T_{in} < T_{sat}$). The coolant maintains liquid state along the channel up to a location where thermodynamic equilibrium quality,

$$x_e = \frac{h - h_f}{h_{fg}}, \tag{4}$$

reaches zero. Thereafter, the flow changes into a saturated two-phase mixture. Figure 2(*a*) illustrates the flow regions of a micro-channel, a single-phase liquid region,

$$L_{sp} = \frac{\rho Q_t c_{P,f}(T_{sat} - T_{in})}{q''_{eff} W}, \tag{5}$$

and a two-phase region, $L_{tp} = L - L_{sp}$. $T_{sat}$ in Eq. (5) is the saturation temperature at the location of $x_e = 0$, which is evaluated using the given heat sink outlet pressure $P_{out}$, assuming a small pressure drop across the heat sink.

The single-phase region can be further divided into developing and fully developed subregions. Since two-phase micro-channel heat sinks feature both low flow rate and small channel size, the flow in the single-phase liquid region is often well within the laminar range. The following equations can be employed to evaluate the length of the two single-phase sub-regions [34]:

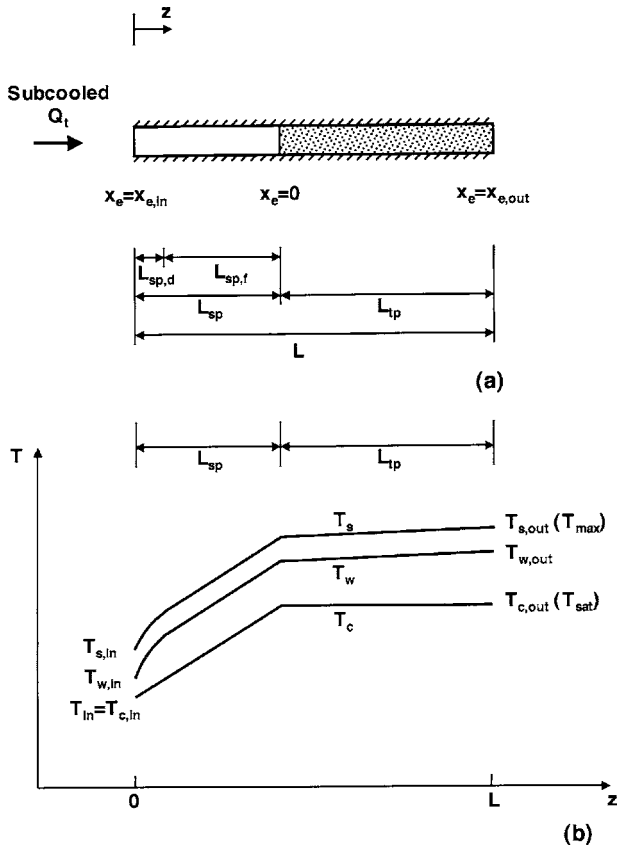


**Fig. 2 (*a*) Flow regions in a micro-channel and (*b*) temperature profile along stream-wise direction**

$$L_{sp,d} = (0.06 + 0.07\beta - 0.04\beta^2)\mathrm{Re}_{in}\, d_h, \tag{6}$$

and

$$L_{sp,f} = L_{sp} - L_{sp,d}. \tag{7}$$

$\Delta P$ is the sum of pressure drops across single-phase and two-phase regions, as well as pressure losses and recoveries associated with the contraction and expansion, respectively, at channel inlet and outlet. The total pressure drop can be expressed as

$$\Delta P = \Delta P_c + \Delta P_{sp,d} + \Delta P_{sp,f} + \Delta P_{tp} + \Delta P_e, \tag{8}$$

where $\Delta P_c$ is the inlet contraction pressure loss, $\Delta P_e$ is the outlet expansion pressure recovery, $\Delta P_{sp,d}$ and $\Delta P_{sp,f}$ denote pressure drops in the single-phase developing and fully developed subregions, respectively, and $\Delta P_{tp}$ is the pressure drop across the two-phase region. $\Delta P_{tp}$ can be further expressed as the sum of accelerational and frictional components:

$$\Delta P_{tp} = \Delta P_{tp,a} + \Delta P_{tp,f}. \tag{9}$$

Predictive tools for evaluating all the pressure drop components in Eqs. (8) and (9) are summarized in Table 1.

**Highest Temperature $T_{max}$.** The performance of an electronic device to which a heat sink is attached is highly temperature dependent. For a given $q''_{eff}$, the highest temperature in the device is encountered immediately below the location of highest temperature in the heat sink. This latter temperature should therefore be kept as low as possible.

Figure 2(*b*) shows the profiles of the coolant mean temperature $T_c$, micro-channel bottom wall temperature $T_w$, and heat sink bottom wall temperature $T_s$ along the streamwise direction. Definitions of these three temperatures are indicated in Fig. 1. In the single-phase region, $T_c$ increases fairly linearly with increasing streamwise distance, and $T_w$ and $T_s$ also increase accordingly. In the two-phase region, however, $T_c$ maintains a fairly constant value equal to $T_{sat}$, and $T_w$ and $T_s$ increase only slightly with distance. This behavior is attributed to the large value of the flow boiling heat transfer coefficient $h_{tp}$ [29]. The highest heat sink temperature is always encountered in the heat sink's bottom wall immediately below the micro-channel outlet. Assuming one-dimensional heat conduction between the heat sink's bottom wall and micro-channel bottom wall, $T_{s,out}$ can be related to the micro-channel bottom wall temperature at the channel outlet by

$$T_{s,out} = T_{w,out} + \frac{q''_{eff} H_w}{k_s}. \tag{10}$$

Since $H_w$ is not part of the optimization methodology and should be made as small as possible, $T_{w,out}$ is used in the present study to represent $T_{max}$:

$$T_{max} = T_{w,out}. \tag{11}$$

**Table 1 Predictive tools for two-phase micro-channel heat sinks**

| | | |
|---|---|---|
| **Pressure drop components** | | |
| $\Delta P_c$ | [35] | $\Delta P_c = \frac{v_f}{2}\left(G^2 - G_{p,in}^2\right) + \frac{K_c v_f}{2} G^2$<br>$K_c = 0.6740 + 1.2501\beta + 0.3417\beta^2 - 0.8358\beta^3;\ \beta = \frac{W_{ch}}{H_{ch}}$<br>For $A_{p,in} \gg N A_{ch}$, $\Delta P_c = \frac{v_f}{2}(1 + K_c)G^2;\ A_{ch} = W_{ch} H_{ch}$ |
| $\Delta P_e$ | [36] | $\Delta P_e = \frac{v_f + x_{e,out} v_{fg}}{2}\left(G_{p,out}^2 - G^2\right) + \frac{K_e\left(v_f + x_{e,out} v_{fg}\right)}{2} G^2$<br>$K_e = \left(1 - \frac{N A_{ch}}{A_{p,out}}\right)^2$<br>For $A_{p,out} \gg N A_{ch}$, $\Delta P_e = 0$ |
| $\Delta P_{sp,f}$ | [34] | $\Delta P_{sp,f} = \frac{2 f_{sp} G^2 L_{sp,f} v_f}{d_h}$<br>$f_{sp} Re_{sp} = 24\left(1 - 1.355\beta + 1.947\beta^2 - 1.701\beta^3 + 0.956\beta^4 - 0.254\beta^5\right);\ Re_{sp} = \frac{G d_h}{\mu_{sp}}$ |
| $\Delta P_{sp,d}$ | [34] | $\Delta P_{sp,d} = \frac{2 f_{sapp} G^2 L_{sp,d} v_f}{d_h}$<br>$f_{sapp} = \frac{1}{Re_{sp}}\left[3.44\left(L_{sp,d}^+\right)^{-0.5} + \frac{K(\infty)/\left(4 L_{sp,d}^+\right) + f_{sp} Re_{sp} - 3.44\left(L_{sp,d}^+\right)^{-0.5}}{1 + C\left(L_{sp,d}^+\right)^2}\right]$<br>$L_{sp,d}^+ = \frac{L_{sp,d}}{Re_{sp} d_h};\ K(\infty) = 0.6740 + 1.2501\beta + 0.3417\beta^2 - 0.8358\beta^3$<br>$C = \left(0.1811 + 4.3488\beta - 1.6027\beta^2\right) \times 10^{-4}$ |
| $\Delta P_{tp,f}$ | [20] | $\Delta P_{tp,f} = \frac{L_{tp}}{x_{e,out}} \int_0^{x_{e,out}} \frac{2 f_f G^2 (1 - x_e)^2 v_f}{d_h} \phi_f^2\, dx_e$<br>$f_f Re_f = 24\left(1 - 1.355\beta + 1.947\beta^2 - 1.701\beta^3 + 0.956\beta^4 - 0.254\beta^5\right);\ Re_f = \frac{G(1 - x_e) d_h}{\mu_f}$<br>$\phi_f^2 = 1 + \frac{C}{X_{tt}} + \frac{1}{X_{tt}^2}$<br>$C = 21\left[1 - \exp\left(-0.319 \times 10^5 d_h\right)\right]\left(0.00418G + 0.0613\right);\ X_{tt} = \left(\frac{\mu_f}{\mu_g}\right)^{0.5}\left(\frac{1 - x_e}{x_e}\right)^{0.5}\left(\frac{v_g}{v_f}\right)^{0.5}$ |
| $\Delta P_{tp,a}$ | [20,37] | $\Delta P_{tp,a} = G^2 v_f\left[\frac{x_{e,out}^2}{\alpha_{out}}\left(\frac{v_g}{v_f}\right) + \frac{(1 - x_{e,out})^2}{1 - \alpha_{out}} - 1\right]$<br>$\alpha_{out} = \frac{1}{1 + \left(\frac{1 - x_{e,out}}{x_{e,out}}\right)\left(\frac{v_f}{v_g}\right)^{2/3}}$ |
| **Heat sink highest temperature** | | |
| $T_{w,out}$ | [21,29] | $T_{w,out} = T_{sat} + \frac{q''_{eff}\left(W_{ch} + W_w\right)}{h_{tp}\left(W_{ch} + 2\eta H_{ch}\right)}$<br>$\eta = \frac{\tanh(m H_{ch})}{m H_{ch}};\ m = \sqrt{\frac{2 h_{sp}}{k_s W_w}}$<br>$h_{tp} = \frac{Nu_3}{Nu_4}\left(E h_{sp}\right)$<br>$Nu_3 = 8.235\left(1 - 1.883\beta + 3.767\beta^2 - 5.814\beta^3 + 5.361\beta^4 - 2.0\beta^5\right)$<br>$Nu_4 = 8.235\left(1 - 2.042\beta + 3.085\beta^2 - 2.477\beta^3 + 1.058\beta^4 - 0.186\beta^5\right)$<br>$h_{sp} = Nu_4 \frac{k_f}{d_h};\ E = 1.0 + 6Bo^{1/16} + f(Bo) x_e^{0.65}$<br>$Bo = \frac{q''_{eff}}{G h_{fg}},\ f(Bo) = -5.3(1 - 855\,Bo)$ |
| **Minimum dissipative heat flux** | | |
| $q''_{min}$ | | $q''_{min} = \frac{\rho Q_t c_{p,f}\left(T_{sat} - T_{in}\right)}{W L}$ |
| **Maximum dissipative heat flux** | | |
| $q''_{max}$ | [33] | $q''_{max} = min\left(q''_{max1}, q''_{max2}\right)$<br>$q''_{max1} = \frac{q''_{p,in} N\left(W_{ch} + 2H_{ch}\right)}{W}$<br>$q''_{p,in} = 33.43\left(G h_{fg}\right)\left(\frac{\rho_g}{\rho_f}\right)^{1.11} We^{-0.21}\left(\frac{L}{d_e}\right)^{-0.36};\ We = \frac{G^2 L}{\sigma \rho_f};\ d_e = \frac{4 W_{ch} H_{ch}}{W_{ch} + 2H_{ch}}$<br>$q''_{max2} = \frac{\rho Q_t\left[c_{p,f}\left(T_{sat} - T_{in}\right) + h_{fg}\right]}{W L}$ |

The fin analysis method is used to evaluate $T_{w,out}$. This method models the solid walls separating micro-channels as thin fins and adopts approximations such as one-dimensional heat conduction and a constant convective heat transfer coefficient along the entire heated perimeter [29]. Applying the fin analysis method to the unit cell shown in Fig. 1 yields the following energy balance at the heat sink outlet,

$$q''_{eff}(W_{ch}+W_w)=h_{tp}(T_{w,out}-T_{sat})(W_{ch}+2\eta H_{ch}), \tag{12}$$

where $h_{tp}$ and $\eta$ are the flow boiling heat transfer coefficient and fin efficiency, respectively. The left-hand side of Eq. (12) represents heat input to the unit cell, and the right-hand side the rate of heat removal by flow boiling from the channel bottom wall and sidewalls. Fin efficiency $\eta$ is evaluated by applying the thin fin approximation to the channel sidewalls,

$$\eta=\frac{\tanh(mH_{ch})}{mH_{ch}}, \tag{13}$$

where $m$ is the fin parameter,

$$m=\sqrt{\frac{2h_{tp}}{k_sW_w}}. \tag{14}$$

$h_{tp}$ is evaluated using the Warrier et al. correlation for micro-channel flow boiling [21]. Other more accurate models can be used to evaluate $h_{tp}$ (e.g., [30]). However, the Warrier et al. correlation is used here because of its relative ease of implementation in the proposed design methodology as well as its reasonable predictive capability [29]. Predictive tools for $T_{w,out}$ are summarized in Table 1.

**Minimum Dissipative Heat Flux $q''_{min}$.** The minimum dissipative heat flux $q''_{min}$ is the lowest heat flux that can sustain flow boiling in the micro-channels. It represents the input heat flux value that causes flow boiling to first occur at the channel outlet and below which any $q''_{eff}$ value would yield single-phase liquid flow throughout the micro-channel. Therefore, $q''_{min}$ is set equal to the dissipative heat flux value corresponding to zero thermodynamic equilibrium quality at the channel outlet, $x_{e,out}=0$. From Eq. (5),

$$L=L_{sp}=\frac{\rho Q_t c_{P,f}(T_{sat}-T_{in})}{q''_{min}W}. \tag{15}$$

Rearranging Eq. (15) yields the relation for $q''_{min}$ given in Table 1.

**Maximum Dissipative Heat Flux $q''_{max}$.** The maximum dissipative heat flux $q''_{max}$ represents maximum value of device heat flux that can be removed by the heat sink. For a two-phase heat sink, $q''_{max}$ is set by the critical heat flux (CHF) in the micro-channels since exceeding this limit would precipitate a sudden large increase in the heat sink temperature, which can lead to permanent device failure. A CHF correlation recently developed by the present authors for two-phase micro-channel heat sinks [33] is used to evaluate $q''_{max}$. At very low coolant flow rates, however, the CHF correlation yields a heat flux value higher than the input heat flux value required to convert all the liquid to saturated vapor at channel outlet, $x_{e,out}=1$. Under these conditions, the input heat flux corresponding to $x_{e,out}=1$ is used for $q''_{max}$. A summary of the predictive relations for $q''_{max}$ is given in Table 1.

## Characteristics of Thermal/Fluid Parameters

A water-cooled copper two-phase micro-channel heat sink with planform dimensions ($W\times L$) of $1\times 1$ cm$^2$ is used to illustrate the general trends of the aforementioned thermal/fluid parameters. Two channel heights are compared, 500 and 1000 $\mu$m. For each $H_{ch}$ value, four ($W_{ch}$,$W_w$) combinations ($50\times 50$,$50\times 100$,$100\times 50$,$100\times 100$ $\mu$m$^2$) are examined. $T_{in}$ and $P_{out}$ are set at 25°C and 1.2 bar, respectively.

Figures 3(*a*)–3(*c*) show the variations of $q''_{max}$ and $q''_{min}$, $\Delta P$, and $T_{w,out}$ with $Q_t$ for $q''_{eff}=100$, 500, and 1000 W/cm$^2$, respectively. On the left side of each figure are the results for the heat sinks with $H_{ch}=1000$ $\mu$m, and on the right side $H_{ch}=500$ $\mu$m.

Figures 3(*a*)–3(*c*) show $q''_{min}$ is a function of $Q_t$ alone and increases with increasing $Q_t$. $q''_{max}$, on the other hand, depends not only on $Q_t$ but micro-channel dimensions ($H_{ch}$, $W_{ch}$, and $W_w$) as well. The dependence of $q''_{max}$ on the micro-channel dimensions will be discussed in a later section. For given micro-channel dimensions, $q''_{max}$ increases with increasing $Q_t$. As discussed earlier, $q''_{min}$ and $q''_{max}$ set lower and upper limits, respectively, for $q''_{eff}$, i.e.,

$$q''_{min}\leqslant q''_{eff}\leqslant q''_{max} \tag{16}$$

for a given $Q_t$. Since both $q''_{min}$ and $q''_{max}$ increase monotonically with increasing $Q_t$, Eq. (16) can be used to determine to minimum and maximum values for $Q_t$ for each set of micro-channel dimensions:

$$Q_{t,min}\leqslant Q_t\leqslant Q_{t,max}, \tag{17}$$

where $Q_{t,min}$ and $Q_{t,max}$ can evaluated from the following relations, respectively:

$$q''_{min}(Q_{t,max})=q''_{eff} \tag{18}$$

and

$$q''_{max}(Q_{t,min})=q''_{eff}. \tag{19}$$

Like $q''_{max}$, $\Delta P$ and $T_{w,out}$ are functions of both $Q_t$ and micro-channel dimensions as illustrated in Figs. 3(*a*)–3(*c*). For fixed micro-channel dimensions, $\Delta P$ decreases with increasing $Q_t$ in the low $Q_t$ region, but could either increase or decrease in the high $Q_t$ region depending on micro-channel dimensions. $T_{w,out}$ increases with increasing $Q_t$ in the low $Q_t$ region, and decreases slightly in the high $Q_t$ region. The dependence of $\Delta P$ and $T_{w,out}$ on micro-channel dimensions will be discussed in a later section.

Comparing the left and right sides of each figure reveals that for the same input parameters as well as $W_{ch}$ and $W_w$, heat sinks with deeper micro-channels (larger $H_{ch}$) always yield better performance by providing lower values for both $\Delta P$ and $T_{w,out}$.

Comparing Figs. 3(*a*)–3(*c*) for different values of $q''_{eff}$ shows a higher $q''_{eff}$ demands a higher $Q_t$ range and yields higher values for both $\Delta P$ and $T_{w,out}$.

The dependence of $q''_{max}$ on micro-channel dimensions is illustrated in Figs. 4(*a*) and 4(*b*). These two figures show constant $q''_{max}$ lines in a $W_{ch}$-$W_w$ plane at $Q_t=120$ ml/min for $H_{ch}=1000$ and 500 $\mu$m, respectively. $q''_{max}$ increases with decreasing $W_{ch}$ and $W_w$ and reaches the highest value at the left lower corner of each plot, i.e., for the lowest $W_{ch}$ and $W_w$ values.

For $Q_t=120$ ml/min, Eq. (15) yields $q''_{min}=667$ W/cm$^2$, independent of $W_{ch}$ or $W_w$. The dashed line corresponding to

$$q''_{max}=q''_{min}=667\ \text{W/cm}^2 \tag{20}$$

in Figs. 4(*a*) and 4(*b*) sets an upper limit for the region of the $W_{ch}$-$W_w$ plane where Eq. (16) is valid, i.e., where $q''_{max}\geqslant q''_{min}$.

Comparing Figs. 4(*a*) and 4(*b*) reveals that for fixed values of $W_{ch}$ and $W_w$ a deeper micro-channel always yields a higher $q''_{max}$ value. This observation further proves that micro-channels should be made as deep as possible, while being mindful of machining and structural limitations.

## Heat Sink Optimal Design

**Design Under Fixed Flow Rate.** Flow rate or pressure drop are key constraints in the design of micro-channel heat sinks since such heat sinks often demand specialized micro-pumps whose performance is dictated by either flow rate or pressure drop.

In this section, optimal design of a two-phase micro-channel heat sink under fixed total volume flow rate $Q_t$ is explored. The water-cooled copper two-phase micro-channel heat sink is again

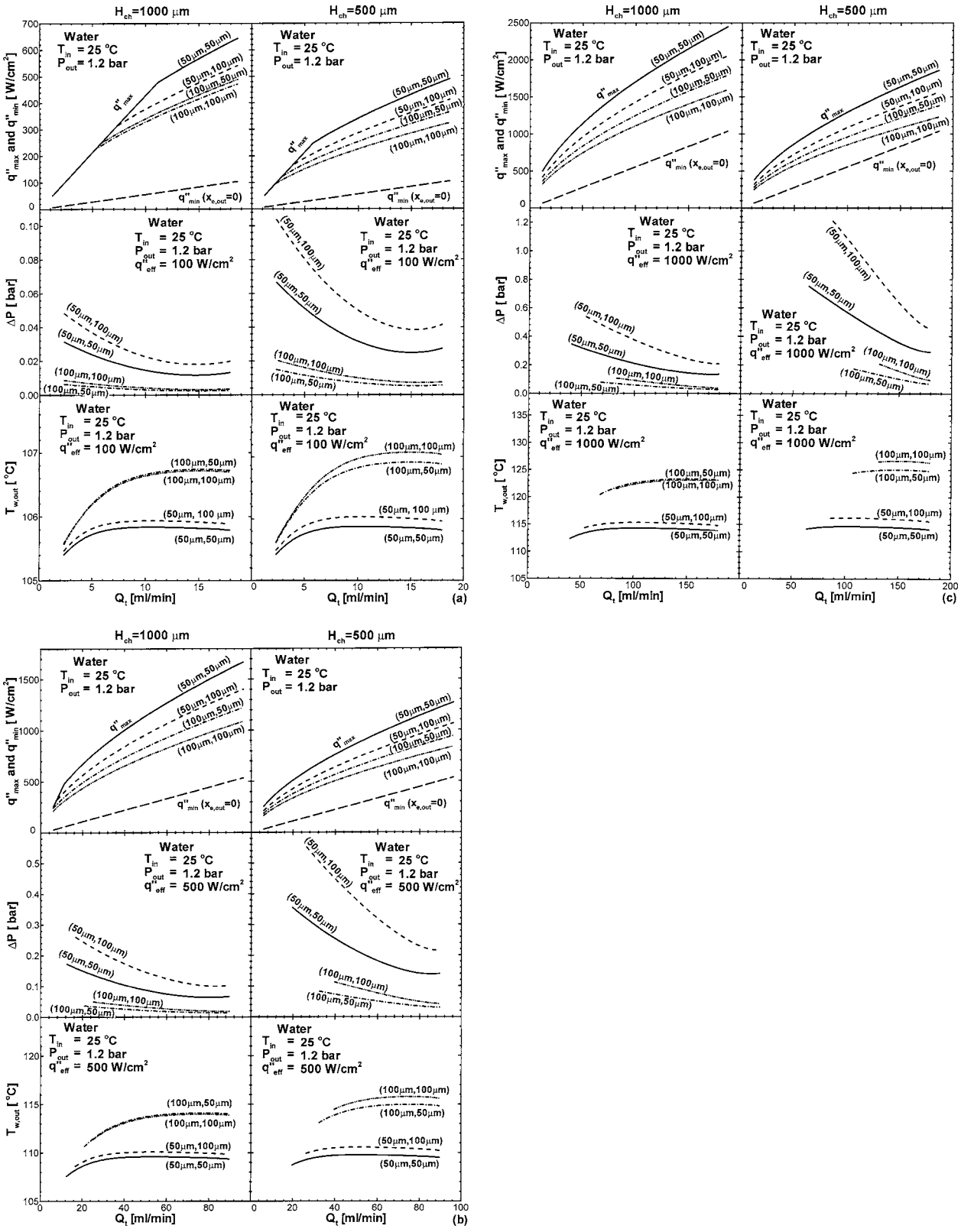


**Fig. 3 Variations of minimum effective heat flux, maximum effective heat flux, pressure drop, and channel bottom temperature at heat sink outlet with total volume flow rate for (*a*) $q''_{eff}$=100 W/cm², (*b*) $q''_{eff}$=500 W/cm², and (*c*) $q''_{eff}$ =1000 W/cm².**

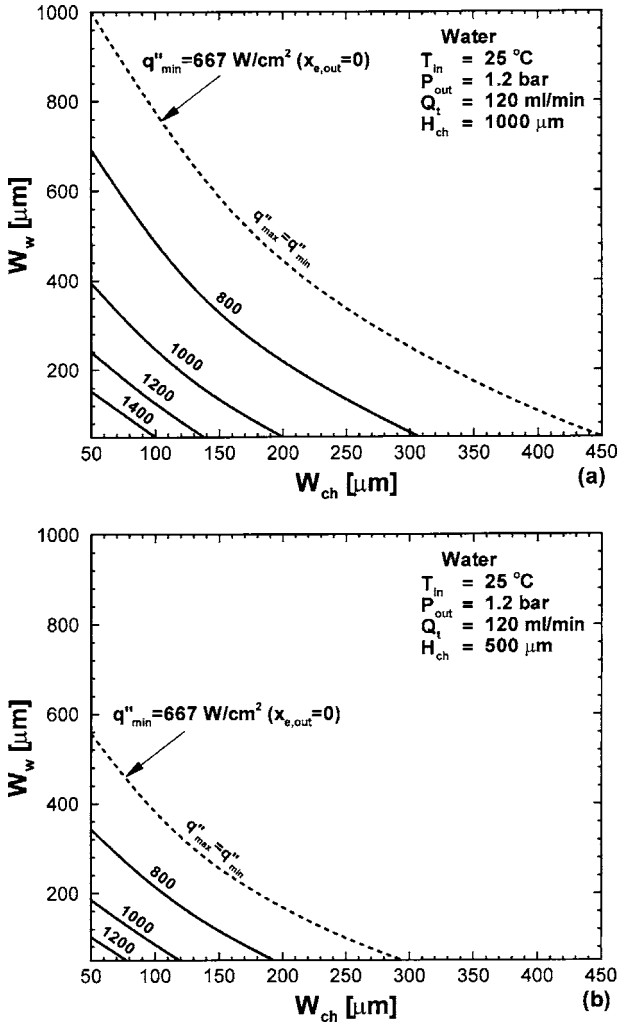


**Fig. 4 Performance map for maximum effective heat flux for (*a*) $H_{ch}$=1000 $\mu$m and (*b*) $H_{ch}$=500 $\mu$m**

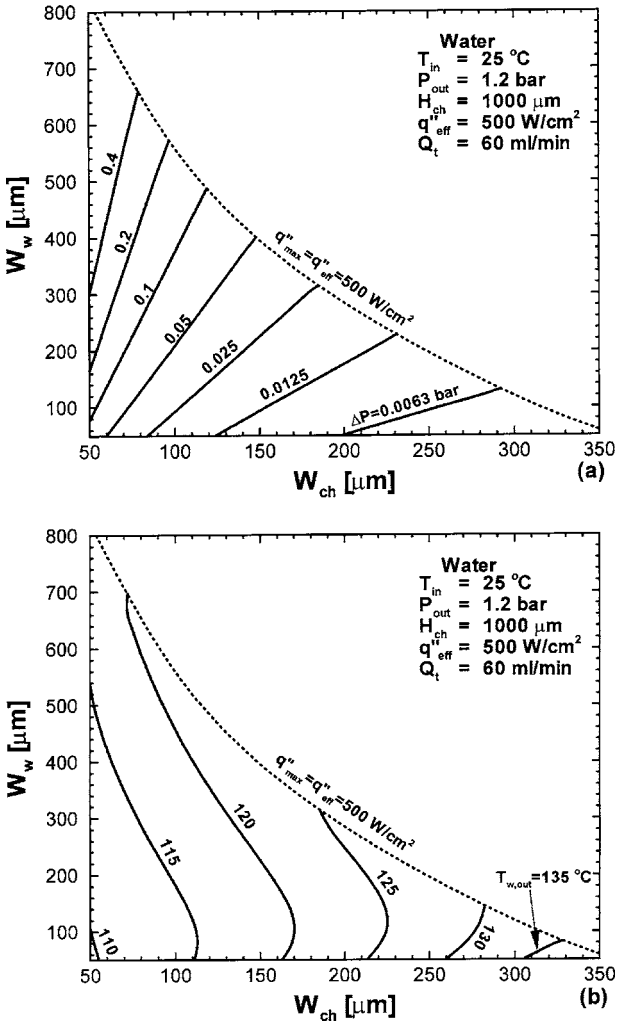


**Fig. 5 Performance map for (*a*) pressure drop and (*b*) channel bottom temperature at heat sink outlet for $q''_{eff}$=500 W/cm² and $Q_t$=60 ml/min**

employed to illustrate the design methodology. Input parameters are summarized as follows: heat sink planform dimensions ($W \times L$) of $1 \times 1$ cm$^2$, $T_{in}$ and $P_{out}$ of 25°C and 1.2 bar, respectively, device heat flux of $q''_{eff}$=500 W/cm$^2$, and a flow rate of $Q_t$ =60 ml/min.

Machining and/or structural limitations should always be examined first to identify maximum channel height $H_{ch,max}$, minimum width, $W_{ch,min}$, and minimum wall thickness, $W_{w,min}$. Another consideration in setting a minimum channel width is the need to avoid clogging.

As discussed in the previous section, deeper micro-channels always produce better performance. Therefore, $H_{ch,max}$ is employed for $H_{ch}$:

$$H_{ch} = H_{ch,max}. \tag{21}$$

Once $H_{ch}$ is fixed, only two other design parameters, $W_{ch}$ and $W_w$, need to be determined, which should satisfy the following relations,

$$W_{ch} \geq W_{ch,min} \tag{22}$$

and

$$W_w \geq W_{w,min}. \tag{23}$$

In the present study, $H_{ch,max}$ is set at 1000 $\mu$m, and both $W_{ch,min}$ and $W_{w,min}$ at 50 $\mu$m. It is important to note that these values generally depend on heat sink material, coolant type, and heat sink fabrication technique; the values used here are intended only to illustrate the use of the optimization methodology.

Although $Q_t$ is an input parameter, it is necessary to make certain $Q_t$ satisfy Eq. (17). Otherwise, a different $Q_t$ value must be assigned from the start. When $Q_{t,min}$ is evaluated from Eq. (19), $H_{ch,max}$, $W_{ch,max}$, and $W_{w,min}$ should be used for micro-channel dimensions as this combination yields the highest possible $q''_{max}$ value, and therefore lowest $Q_{t,min}$.

Figures 5(*a*) and 5(*b*) show the output of the optimization methodology in a $W_{ch}$-$W_w$ plane. For a fixed flow rate of $Q_t$ =60 ml/min and a device heat flux of $q''_{eff}$=500 W/cm$^2$, the acceptable range of two-phase operation is confined to the region below the dashed line corresponding to $q''_{max}=q''_{eff}$=500 W/cm$^2$ since only $(W_{ch}, W_w)$ combinations that are located in this region satisfy the requirement $q''_{eff} < q''_{max}$. In the case where a factor of safety on CHF needs to be assigned, the acceptable design region is obtained in a similar manner using the line corresponding to $q''_{max}=\Phi q''_{eff}$, where $\Phi$ is the factor of safety on CHF.

The next step involves evaluating $\Delta P$ and $T_{w,out}$ corresponding to micro-channel dimensions in the acceptable design region. Predictive tools given Table 1 are employed to conduct the evaluation. Figures 5(*a*) and 5(*b*) show lines of constant $\Delta P$ and constant $T_{w,out}$, respectively. Figure 5(*a*) shows $\Delta P$ is low for large $W_{ch}$ and

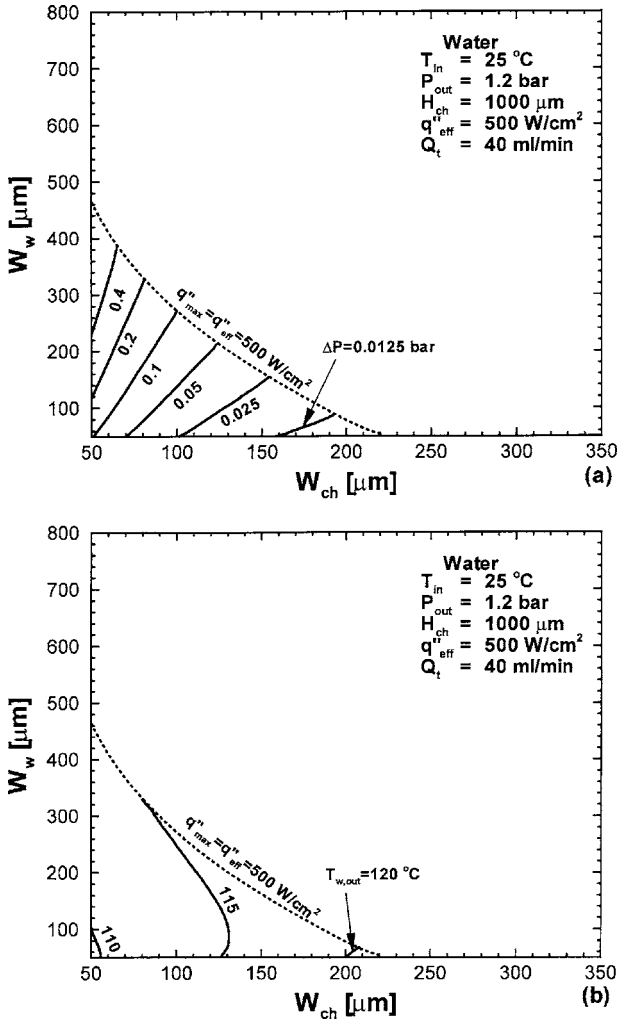


**Fig. 6 Performance map for (*a*) pressure drop and (*b*) channel bottom temperature at heat sink outlet for $q''_{eff}$=500 W/cm² and $Q_t$=40 ml/min**

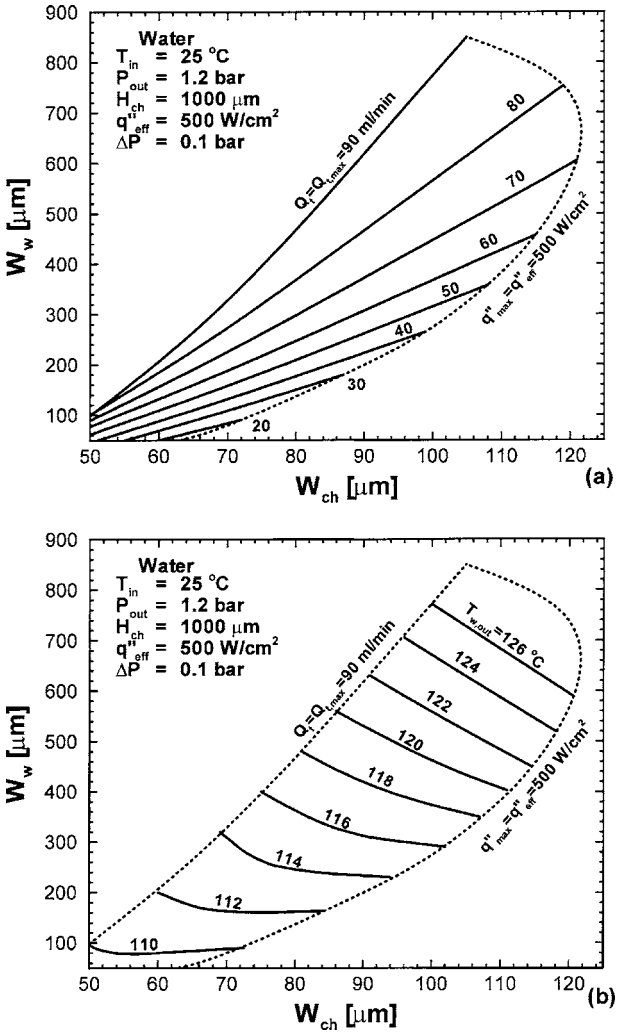


**Fig. 7 Performance map for (*a*) total volume flow rate and (*b*) channel bottom temperature at heat sink outlet for $q''_{eff}$ =500 W/cm² and $\Delta P$=0.1 bar**

small $W_w$ and increases with decreasing $W_{ch}$ and increasing $W_w$. Figure 5(*b*), on the other hand, shows $T_{w,out}$ is low for small $W_{ch}$ and small $W_w$ and increases with increasing $W_{ch}$.

Figures 6(*a*) and 6(*b*) show similar plots corresponding to a lower flow rate of $Q_t$=40 ml/min. The general trends in these figures are similar to those of Figs. 5(*a*) and 5(*b*), respectively, except that the $q''_{max}$ limit is shifted towards smaller channel dimensions. Comparing Figs. 5(*a*) and 6(*a*) reveals that for the same micro-channel dimensions, $\Delta P$ increases with decreasing $Q_t$. This is because the pressure drop in the two-phase region is higher than in the single-phase region. With a lower flow rate, two-phase flow occupies a larger portion of the micro-channel length, resulting in higher total pressure drop. A comparison of Figs. 5(*b*) and 6(*b*) shows $T_{w,out}$ decreases with decreasing $Q_t$. These trends are valid only for low values of $Q_t$; high $Q_t$ values are expected to yield the opposite trend as shown in Figs. 3(*a*)–3(*c*).

Figures such as 5(*a*), 5(*b*), 6(*a*), and 6(*b*) are the final output of the numerical optimization procedure. They provide the end user with an acceptable range of $(W_{ch}, W_w)$ combinations which can safely remove the heat for a given flow rate. The heat sink designer is left with the decision to select an acceptable combination of $\Delta P$ and $T_{w,out}$; this latter combination dictates the dimensions ($W_{ch}$ and $W_w$) of the micro-channel.

**Design Under Fixed Pressure Drop.** In some applications, optimal design of a two-phase micro-channel heat sink must be performed under the requirement of a fixed pressure drop $\Delta P$, instead of a fixed flow rate $Q_t$. This section outlines the design procedure corresponding to a fixed $\Delta P$. Input parameters discussed here are identical to those in the previous section with the exception that $Q_t$ is now an output variable and pressure drop is fixed at $\Delta P$ =0.1 bar.

The design procedure is very similar to that discussed in the previous section. As indicated in Figs. 7(*a*) and 7(*b*), the acceptable design region under fixed $\Delta P$ is enveloped by lines corresponding to $Q_t=Q_{t,max}$=90 ml/min and $q''_{max}=q''_{eff}$=500 W/cm². Lines corresponding to constant values of $Q_t$ and $T_{w,out}$ are constructed in Figs. 7(*a*) and 7(*b*), respectively, within the acceptable design region.

Figures 8(*a*) and 8(*b*) show similar plots for a higher pressure drop of $\Delta P$=0.2 bar. The general trends in these plots are similar to those of Figs. 7(*a*) and 7(*b*) except that the acceptable design region is shifted to lower $W_{ch}$ and high $W_w$ values.

Figures such as 7(*a*), 7(*b*), 8(*a*), and 8(*b*) are the final output of the numerical optimization corresponding to a fixed $\Delta P$. The heat sink designer is left with the decision to select an acceptable combination of $Q_t$ and $T_{w,out}$ based upon which the channel dimensions ($W_{ch}$ and $W_w$) are determined.

**Summary of Optimization Procedure.** Figure 9 shows a flow

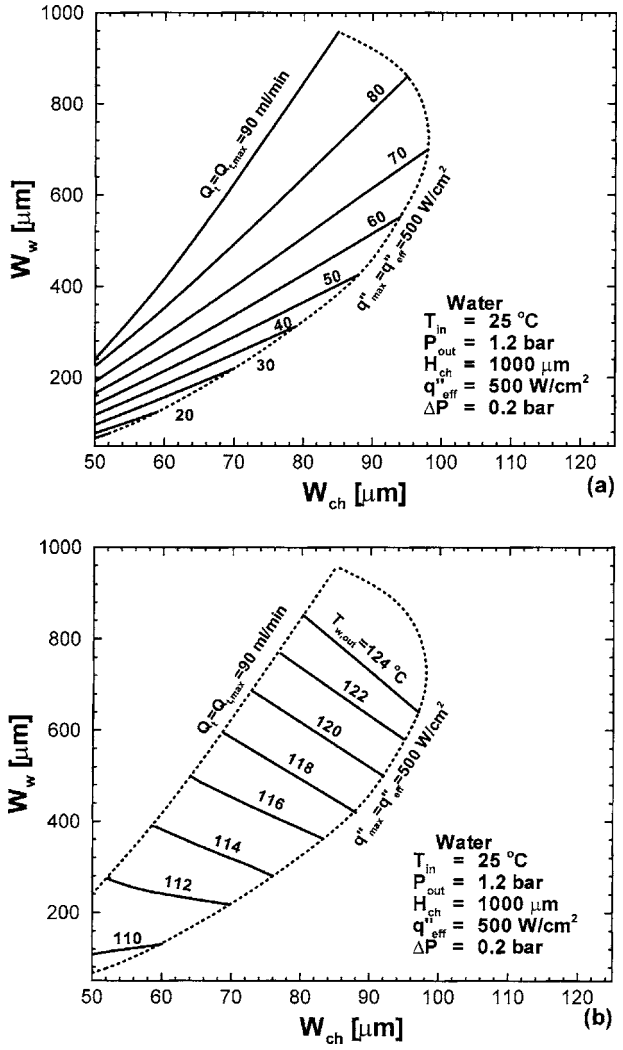


**Fig. 8 Performance map for (*a*) total volume flow rate and (*b*) channel bottom temperature at heat sink outlet for $q''_{eff}$ =500 W/cm² and $\Delta P$=0.2 bar**

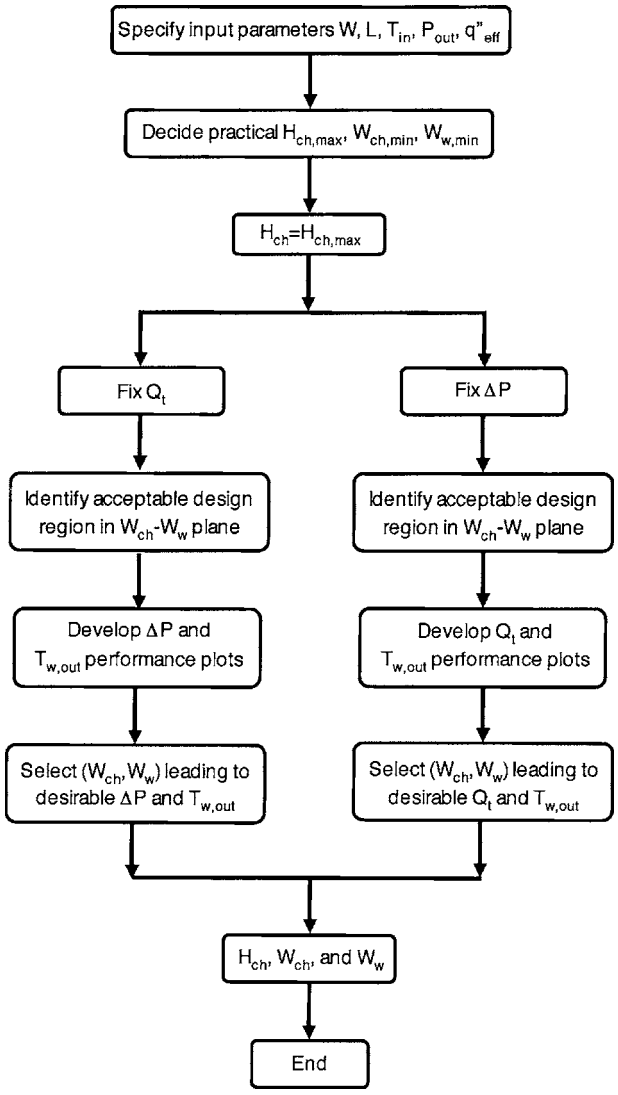


**Fig. 9 Flow chart of numerical procedure for optimal design of two-phase micro-channel heat sink**

chart that summarizes the numerical procedure for optimal design of a two-phase micro-channel heat sink under fixed total volume flow rate or fixed pressure drop. Figures 10(*a*) and 10(*b*) illustrate the general trends of output parameters within the acceptable design region for fixed total volume flow rate and fixed pressure drop, respectively.

## Conclusions

This study concerns optimal design of two-phase micro-channel heat sinks. System parameters and predictive tools were first summarized and are followed by a discussion of the characteristics of thermal/fluid transport parameters. Finally, a systematic optimization methodology for heat sink design was developed for the conditions of either fixed total volume flow rate or fixed pressure drop. Key findings from the study are as follows:

1. System parameters associated with two-phase micro-channel heat sinks can be grouped into geometrical parameters, operating parameters, and thermal/fluid parameters. Geometrical parameters include heat sink and micro-channel dimensions. In heat sink design, heat sink dimensions and operating parameters are used as input parameters and are often specified beforehand. Thermal/fluid parameters are output parameters that describe the transport behavior of the heat sink and whose magnitude is used to guide the designer in selecting optimum micro-channel dimensions.
2. With the exception of minimum dissipative heat flux required to initiate boiling at the channel outlet, all other thermal/fluid parameters are sensitive to micro-channel dimensions.
3. A design procedure for two-phase micro-channel heat sinks under the conditions of a fixed device heat flux and fixed total volume flow rate is developed. This procedure yields an acceptable design region encompassing all possible micro-channel dimensions and provides predictions for pressure drop and highest heat sink temperature from which a designer can select optimum channel dimensions.
4. A similar design procedure is proposed for the conditions of fixed device heat flux and fixed pressure drop. This procedure is used to select optimum channel dimensions that yield acceptable values for flow rate and highest heat sink temperature.

## Acknowledgment

The authors are grateful for the support of the Office of Basic Energy Sciences of the U.S. Department of Energy (Award No. DE-FG02-93ER14394 A7).

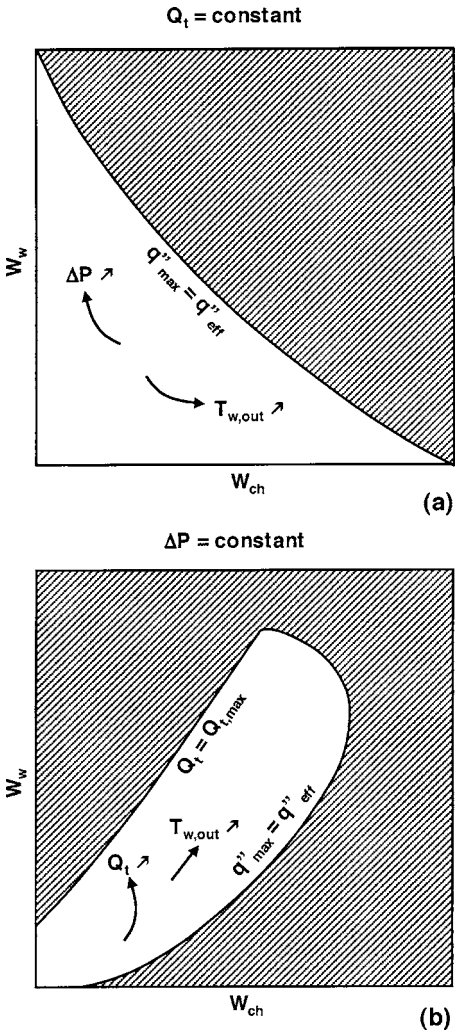


**Fig. 10 General performance map trends for (*a*) fixed total volume flow rate and (*b*) fixed pressure drop**

## Nomenclature

$A_{ch}$ = cross-sectional area of micro-channel
$A_p$ = cross-sectional area of plenum
Bo = boiling number
$C$ = parameter in pressure drop relations
$c_P$ = specific heat at constant pressure
$d_e$ = heated equivalent diameter
$d_h$ = hydraulic diameter of micro-channel
$E$ = parameter in heat transfer relations
$f$ = friction factor
$f_{app}$ = apparent friction factor for developing single-phase liquid flow
$f_f$ = friction factor based on local liquid flow rate
$f_{sp}$ = friction factor in single-phase fully developed region
$G$ = mass velocity
$h$ = enthalpy
$h_f$ = enthalpy of saturated liquid
$h_{fg}$ = latent heat of vaporization
$h_{sp}$ = single-phase convective heat transfer coefficient
$h_{tp}$ = flow boiling heat transfer coefficient
$H$ = height of heat sink
$H_c$ = cover plate thickness
$H_{ch}$ = height of micro-channel
$H_w$ = distance from micro-channel bottom wall to heat sink bottom wall
$k$ = thermal conductivity
$K(\infty)$ = entrance loss coefficient
$K_c$ = contraction loss coefficient
$K_e$ = expansion recovery coefficient
$L$ = length of heat sink
$L_{sp}$ = length of single-phase region
$L^+_{sp,d}$ = nondimensional length of single-phase developing subregion
$L_{sp,d}$ = length of single-phase developing subregion
$L_{sp,f}$ = length of single-phase fully developed subregion
$L_{tp}$ = length of two-phase region
$m$ = fin parameter
$N$ = number of micro-channels in heat sink
$\mathrm{Nu}_3, \mathrm{Nu}_4$ = Nusselt number for laminar fully developed flow for three and four wall heat transfer
$P$ = pressure
$P_{out}$ = outlet pressure
$P_w$ = total rate of heat supplied to heat sink
$\Delta P$ = pressure drop across heat sink
$\Delta P_c$ = contraction pressure loss
$\Delta P_e$ = expansion pressure recovery
$\Delta P_{sp,d}$ = pressure drop in single-phase developing subregion
$\Delta P_{sp,f}$ = pressure drop in single-phase fully developed subregion
$\Delta P_{tp}$ = pressure drop in two-phase region
$\Delta P_{tp,a}$ = accelerational two-phase pressure drop
$\Delta P_{tp,f}$ = frictional two-phase pressure drop
$q''_{eff}$ = dissipative heat flux based on heat sink planform area
$q''_{max}$ = maximum dissipative heat flux
$q''_{min}$ = minimum dissipative heat flux
$q''_p$ = mean heat flux over heated inside area of micro-channel
$Q_t$ = total volume flow rate
$Q_{t,max}$ = maximum total volume flow rate
$Q_{t,min}$ = minimum total volume flow rate
Re = Reynolds number
$\mathrm{Re}_f$ = Reynolds number based on local liquid flow rate
$\mathrm{Re}_{in}$ = Reynolds number based on inlet liquid conditions
$\mathrm{Re}_{sp}$ = Reynolds number based on properties at mean temperature in single-phase liquid region
$T$ = temperature
$T_c$ = coolant mean temperature
$T_{in}$ = inlet temperature
$T_{max}$ = highest temperature in optimization procedure ($T_{max}=T_{w,out}$)
$T_s$ = heat sink bottom wall temperature
$T_{sat}$ = saturation temperature
$T_w$ = micro-channel bottom wall temperature
$v$ = specific volume
$v_{fg}$ = specific volume difference between saturated liquid and saturated vapor
$W$ = width of heat sink
$W_{ch}$ = width of micro-channel
$W_e$ = weber number
$W_w$ = thickness of wall separating micro-channels
$x_e$ = thermodynamic equilibrium quality
$x_{e,out}$ = thermodynamic equilibrium quality at channel outlet
$X_{vv}$ = Martinelli parameter for laminar liquid-laminar vapor flow
$z$ = stream-wise distance

### Greek Symbols

$\alpha$ = void fraction
$\beta$ = aspect ratio of micro-channel
$\phi_f^2$ = two-phase frictional multiplier based on local liquid flow rate
$\Phi$ = factor of safety on CHF
$\eta$ = fin efficiency
$\mu$ = viscosity
$\rho$ = density
$\sigma$ = surface tension

### Subscripts

$f$ = liquid
$g$ = vapor
$in$ = inlet
$max$ = maximum
$min$ = minimum
$out$ = outlet
$p$ = inlet or outlet plenum
$s$ = base substrate
$sp$ = single-phase liquid
$sp,d$ = single-phase developing subregion
$sp,f$ = single-phase fully developed subregion
$tp$ = two phase

## References


[1] Tuckerman, D. B., and Pease, R. F. W., 1981, "High-Performance Heat Sinking for VLSI," IEEE Electron Device Lett., **EDL-2**, pp. 126–129.
[2] Kishimito, T., and Ohsaki, T., 1986, "VLSI Packaging Technique Using Liquid-Cooled Channels," IEEE Trans. Compon., Hybrids, Manuf. Technol., **CHMT-9**, pp. 328–335.
[3] Rahman, M. M., and Gui, F., 1993, "Experimental Measurements of Fluid Flow and Heat Transfer in Microchannel Cooling Passages in a Chip Substrate," ASME J. Electron. Packag., **EEP-4**, pp. 495–506.
[4] Ravigururajan, T. S., Cuta, J., McDonald, C. E., and Drost, M. K., 1996, "Single-Phase Flow Thermal Performance Characteristics of a Parallel Micro-Channel Heat Exchanger," *Proceedings of National Heat Transfer Conference*, ASME HTD-329, Vol. 7, pp. 157–166.
[5] Kawano, K., Minakami, K., Iwasaki, H., and Ishizuka, M., 1998, "Micro Channel Heat Exchanger for Cooling Electrical Equipment," *Proceedings of the ASME Heat Transfer Division*, ASME HTD-361–3/PID-3, pp. 173–180.
[6] Harms, T. M., Kazmierczak, M. J., and Cerner, F. M., 1999, "Developing Convective Heat Transfer in Deep Rectangular Microchannels," Int. J. Heat Fluid Flow, **20**, pp. 149–157.
[7] Qu, W., and Mudawar, I., 2002, "Experimental and Numerical Study of Pressure Drop and Heat Transfer in a Single-Phase Micro-Channel Heat Sink," Int. J. Heat Mass Transfer, **45**, pp. 2549–2565.
[8] Knight, R. W., Goodling, J. S., and Hall, D. J., 1991, "Optimal Thermal Design of Forced Convection Heat Sinks—Analytical," ASME J. Electron. Packag., **113**, pp. 313–321.
[9] Knight, R. W., Hall, D. J., Goodling, J. S., and Jaeger, R. C., 1992, "Heat Sink Optimization with Application to Microchannels," IEEE Trans. Compon., Hybrids, Manuf. Technol., **15**, pp. 832–842.
[10] Lee, D. Y., and Vafai, K., 1999, "Comparative Analysis of Jet Impingement and Microchannel Cooling for High Heat Flux Applications," Int. J. Heat Mass Transfer, **42**, pp. 1555–1568.
[11] Choquette, S. F., Faghri, M., Charmchi, M., and Asako, Y., 1996, "Optimum Design of Microchannel Heat Sinks," *Micro-Electro-Mechanical Systems (MEMS)—1996*, DSC-Vol. 59, ASME, pp. 115–126.
[12] Kennedy, J. E., Roach, G. M., Jr., Dowling, M. F., Abdel-Khalik, S. I., Ghiaasiaan, S. M., Jeter, S. M., and Quershi, Z. H., 2000, "The Onset of Flow Instability in Uniformly Heated Horizontal Microchannels," ASME J. Heat Transfer, **122**, pp. 118–125.
[13] Qu, W., and Mudawar, I., 2002, "Prediction and Measurement of Incipient Boiling Heat Flux in Micro-Channel Heat Sinks," Int. J. Heat Mass Transfer, **45**, pp. 3933–3945.
[14] Zhang, L., Koo, J. M., Jiang, L., Banerjee, S. S., Ashegi, M., Goodson, K. E., Santiago, J. G., and Kenny, T. W., 2000, "Measurement and Modeling of Two-Phase Flow in Microchannels with Nearly-Constant Heat Flux Boundary Conditions," *Micro-Electro-Mechanical Systems (MEMS)—2000*, A. Lee et al., eds., ASME, MEMS-Vol. 2, pp. 129–135.
[15] Jiang, L., Wong, M., and Zohar, Y., 2001, "Forced Convection Boiling in a Microchannel Heat Sink," J. Microelectromech. Syst., **10**, pp. 80–87.
[16] Qu, W., and Mudawar, I., 2004, "Transport Phenomena in Two-Phase Micro-Channel Heat Sinks," ASME J. Electron. Packag., **126**, pp. 213–224.
[17] Kandlikar, S. G., Steinke, M. E., Tian, S., and Campbell, L. A., 2001, "High-Speed Photographic Observation of Flow Boiling of Water in Parallel Mini-Channels," *Proceedings of National Heat Transfer Conference*, ASME, pp. 675–684.
[18] Hetsroni, G., Mosyak, A., Segal, Z., and Ziskind, G., 2002, "A Uniform Temperature Heat Sink for Cooling of Electronic Devices," Int. J. Heat Mass Transfer, **45**, pp. 3275–3286.
[19] Wu, H. Y., and Cheng, P., 2003, "Visualization and Measurements of Periodic Boiling in Silicon Microchannels," Int. J. Heat Mass Transfer, **46**, pp. 2603–2614.
[20] Qu, W., and Mudawar, I., 2003, "Measurement and Prediction of Pressure Drop in Two-Phase Micro-Channel Heat Sinks," Int. J. Heat Mass Transfer, **46**, pp. 2737–2753.
[21] Warrier, G. R., Dhir, V. K., and Momoda, L. A., 2002, "Heat Transfer and Pressure Drop in Narrow Rectangular Channel," Exp. Therm. Fluid Sci., **26**, pp. 53–64.
[22] Bowers, M. B., and Mudawar, I., 1994, "High Flux Boiling in Low Flow Rate, Low Pressure Drop Mini-Channel and Micro-Channel Heat Sinks," Int. J. Heat Mass Transfer, **37**, pp. 321–332.
[23] Bowers, M. B., and Mudawar, I., 1994, "Two-Phase Electronic Cooling Using Mini-Channel and Micro-Channel Heat Sinks: Part 1—Design Criteria and Heat Diffusion Constraints," ASME J. Electron. Packag., **116**, pp. 290–297.
[24] Bowers, M. B., and Mudawar, I., 1994, "Two-Phase Electronic Cooling Using Mini-Channel and Micro-Channel Heat Sinks: Part 2—Flow Rate and Pressure Drop Constraints," ASME J. Electron. Packag., **116**, pp. 298–305.
[25] Tran, T. N., Chyu, M. C., Wambsganss, M. W., and France, D. M., 2000, "Two-Phase Pressure Drop of Refrigerants During Flow Boiling in Small Channels: An Experimental Investigation and Correlation Development," Int. J. Multiphase Flow, **26**, pp. 1739–1754.
[26] Lee, H. J., and Lee, S. Y., 2001, "Heat Transfer Correlation for Boiling Flows in Small Rectangular Horizontal Channels With Low Aspect Ratios," Int. J. Multiphase Flow, **27**, pp. 2043–2062.
[27] Peng, X. F., and Wang, B. X., 1993, "Forced Convection and Flow Boiling Heat Transfer for Liquid Flowing Through Microchannels," Int. J. Heat Mass Transfer, **36**, pp. 3421–3427.
[28] Ravigururajan, T. S., 1998, "Impact of Channel Geometry on Two-Phase Flow Heat Transfer Characteristics of Refrigerants in Microchannel Heat Exchangers," ASME J. Heat Transfer, **120**, pp. 485–491.
[29] Qu, W., and Mudawar, I., 2003, "Flow Boiling Heat Transfer in Two-Phase Micro-Channel Heat Sinks-I. Experimental Investigation and Assessment of Correlation Methods," Int. J. Heat Mass Transfer, **46**, pp. 2755–2771.
[30] Qu, W., and Mudawar, I., 2003, "Flow Boiling Heat Transfer in Two-Phase Micro-Channel Heat Sinks-II. Annular Two-Phase Flow Model," Int. J. Heat Mass Transfer, **46**, pp. 2773–2784.
[31] Roach, G. M., Jr., Abdel-Khalik, S. I., Ghiaasiaan, S. M., Dowling, M. F., and Jeter, S. M., 1999, "Low-Flow Critical Heat Flux in Heated Microchannels," Nucl. Sci. Eng., **131**, pp. 411–425.
[32] Yu, W., France, D. M., Wambsganss, M. W., and Hull, J. R., 2002, "Two-Phase Pressure Drop, Boiling Heat Transfer, and Critical Heat Flux to Water in a Small-Diameter Horizontal Tube," Int. J. Multiphase Flow, **28**, pp. 927–941.
[33] Qu, W., and Mudawar, I., 2004, "Measurement and Correlation of Critical Heat Flux in Two-Phase Micro-Channel Heat Sinks," Int. J. Heat Mass Transfer, **47**, pp. 2045–2059.
[34] Shah, R. K., and London, A. L., 1978, *Laminar Flow Forced Convection in Ducts: A Source Book for Compact Heat Exchanger Analytical Data*, Suppl. 1, Academic Press, New York.
[35] Blevins, R. D., 1984, *Applied Fluid Dynamics Handbook*, Van Nostrand Reinhold Company, New York.
[36] Collier, J. G., and Thome, J. R., 1994, *Convective Boiling and Condensation*, 3rd ed., Oxford University Press, Oxford.
[37] Zivi, S. M., 1964, "Estimation of Steady-State Steam Void-Fraction by Means of the Principle of Minimum Entropy Production," ASME J. Heat Transfer, **86**, pp. 247–252.